PHILOSOPHICAL TRANSACTIONS OF THE ROYAL SOCIETY A MATHEMATICAL, PHYSICAL & ENGINEERING SCIENCES

Gravity-Field Determination from Laser Observations [and Discussion]

E. M. Gaposchkin and J. A. Weightman

Phil. Trans. R. Soc. Lond. A 1977 **284**, 515-527
doi: 10.1098/rsta.1977.0027

Phil. Trans. R. Soc. Lond. A. **284**, 515–527 (1977) [515]
Printed in Great Britain

Gravity-field determination from laser observations

By E. M. Gaposchkin
Smithsonian Astrophysical Observatory, Cambridge, Massachusetts 02138, *U.S.A.*

Knowledge of long-wavelength features of the geopotential is significantly improved by the use of precision satellite tracking with lasers. Tracking data on nine satellites are combined with terrestrial gravimetry to obtain a spherical-harmonics representation of the geopotential complete through degree and order 24. An improved gravity-field model provides better satellite ephemerides and a reference for analysing satellite-to-sea-surface altimetry.

1. Introduction

Satellite-tracking data have been successfully used for many years in the determination of fundamental geodetic parameters, including both the geopotential and geocentric station coordinates (see, for example, Mueller 1974; Anderle 1974; Gaposchkin 1974; Schmid 1974; Smith *et al.* 1975). All these analyses have relied mostly on data with an accuracy of only 10 m or poorer. Nevertheless, results have been obtained with an inherent accuracy of better than 5 m. More precise data are now becoming available in sufficient quantity to allow a redetermination of these fundamental geodetic parameters with improved accuracy. These data are coming from pulsed ranging lasers that track satellites equipped with reflecting cube-corner arrays. Data now being analysed apparently have an accuracy of better than 10 cm, which will lead to a 100-fold improvement in our knowledge of geodetic parameters and other geophysical quantities.

The objective of this work is to obtain a global representation of the geopotential in spherical harmonics with sufficient detail to determine both a satellite trajectory and the geocentric coordinates of all the tracking stations in a well-defined coordinate system to an accuracy of a few centimetres or better. Both objectives are achieved by analysing satellite-tracking laser data in combination with other data. The global nature of the analysis requires coordinated observations from stations in a worldwide network.

Since the data are acquired by several agencies operating in concert, those chosen for analysis are taken from periods of cooperative tracking programs covering several years. This results in an inhomogeneous data set with variable accuracy. Finally, laser tracking data, no matter how accurate, cannot give a uniform description of the gravity field expressed in spherical harmonics, nor can they provide a well-defined reference frame. Therefore, for the moment, terrestrial gravimetry and simultaneous camera observations are also used.

In parallel with the increased accuracy of tracking data, improvements in the treatment of the orbital-perturbation theory and geophysical phenomena have been realized. For example, the inclination function for tesseral-harmonics perturbations as formulated by Kaula (1966) computationally loses accuracy for high degrees and has been replaced by the equivalent formula derived from group theory (Gaposchkin 1973). The interaction between J_2 and resonant harmonics has likewise been improved. Lunar and solar perturbations, body tides, and ocean tides have been computed to the necessary accuracy (Kozai 1973). Perturbations arising from the non-inertialness of the adopted coordinate system have been corrected and improved (Kinoshita 1975, 1976), and those due to direct solar radiation pressure (Aksnes 1976), albedo pressure (Lautman 1976*a*, *b*), and infrared radiation (Lautman 1976*c*) have all been included and tested (Gaposchkin, Latimer & Mendes 1975). Particular attention has been paid to the relation between the semimajor axis a and the mean motion n – i.e. the modified Kepler third law – because laser data are a direct materialization of scale. Eventually, when other errors are reduced, laser data will be used to determine GM from observations of n and a. For the moment, we adopt the value of GM from Esposito & Ng (1975) (see table 1) and pay particular attention to possible distortions due to inadequate modelling of Kepler's third law or to an error in the adopted value of GM.

Table 1. Constants used in orbital computations

$GM = 3.986005 \times 10^{14}$ m³ s⁻² → $GM = 3.986005 \times 10^{14}\ \mathrm{m^3\ s^{-2}}$

$c = 2.997925 \times 10^{8}\ \mathrm{m\ s^{-1}}$ = speed of light

$k_2 = 0.29$ = Love's number for solar and lunar body tides

$k_2' = -0.30$

$k_4' = -0.13$

$k_6' = -0.09$

$\epsilon_2 = 0°$ = phase lag of tide

*M*2 ocean tide

l	m	amplitude	phase
2	2	4.4 cm	−30°
4	2	1.2 cm	−167°
6	2	0.08 cm	97°

*S*2 ocean tide

l	m	amplitude	phase
2	2	2.0 cm	−30°
4	2	0.5 cm	−167°
6	2	0.04 cm	97°

$a_e = 6.378140$ Mm

$\alpha = 0.32$ = Earth's albedo

satellite	$\dfrac{A/m}{\mathrm{cm^2\ g^{-1}}}$
7010901	0.20
6701401	0.30
6701101	0.30
6503201	0.13
7501001	0.009
6508901	0.10
7502701	0.04
6800201	0.06
6406401	0.10

The basic constants adopted for the orbit computation are given in table 1. The values of GM and c define the scale of the orbit and the terrestrial system. An improved value of

$$c = 2.997\,924\,58 \times 10^{8}\,\mathrm{m\,s^{-1}}$$

will be used in future analysis. In fact, this improved value is consistent with the adopted value of GM, but the one part per 7 million scale distortion introduced with the adopted value is much smaller than other errors at this time. For the final orbital results reported here, the periodic perturbations due to body tides and ocean tides are computed from the coefficients in table 1.

The area-to-mass ratios (A/m) used for computation of solar radiation pressure and albedo perturbations have been empirically determined from analysis of long-term variations of mean orbital elements, principally the eccentricity and the semimajor axis. As indicated, all these parameters (except c) will be revised by laser tracking data. The zonal harmonics are held fixed at the values given in Gaposchkin (1973).

Generally speaking, the mathematical treatment of orbital perturbations is a complicated and subtle business, and a continuing effort is needed. The benefits of analytical treatment in terms of insight and efficiency are manifest.

Table 2. Laser stations used in this analysis

station			data-acquisition campaign		
number	location	operating agency	ISAGEX 1971	EPSOC/SAFE 1972–74	Geos 3 1975
7902	Olifantsfontein, S. Africa	SAO	×	×	×
7907	Arequipa, Peru	SAO	×	×	×
7921	Mt Hopkins, Arizona	SAO	×	×	×
7929	Natal, Brazil	SAO	×	×	×
7930, 7940	Athens, Greece	SAO	×	×	×
7050, 7063	GSFC, Maryland	NASA	×	×	×
7060	Guam Island	NASA	×	.	.
7061	San Diego, California	NASA	.	×	.
7080	Quincy, California	NASA	.	×	.
7067	Bermuda Island	NASA	.	.	×
7068	Grand Turk Island	NASA	.	.	×
7804	San Fernando, Spain	CNES	×	.	.
7809	Haute Provence, France	CNES	×	.	.
7819	Grand Canary Island	CNES	.	.	×
7842	Grasse, France	CNES	.	.	×

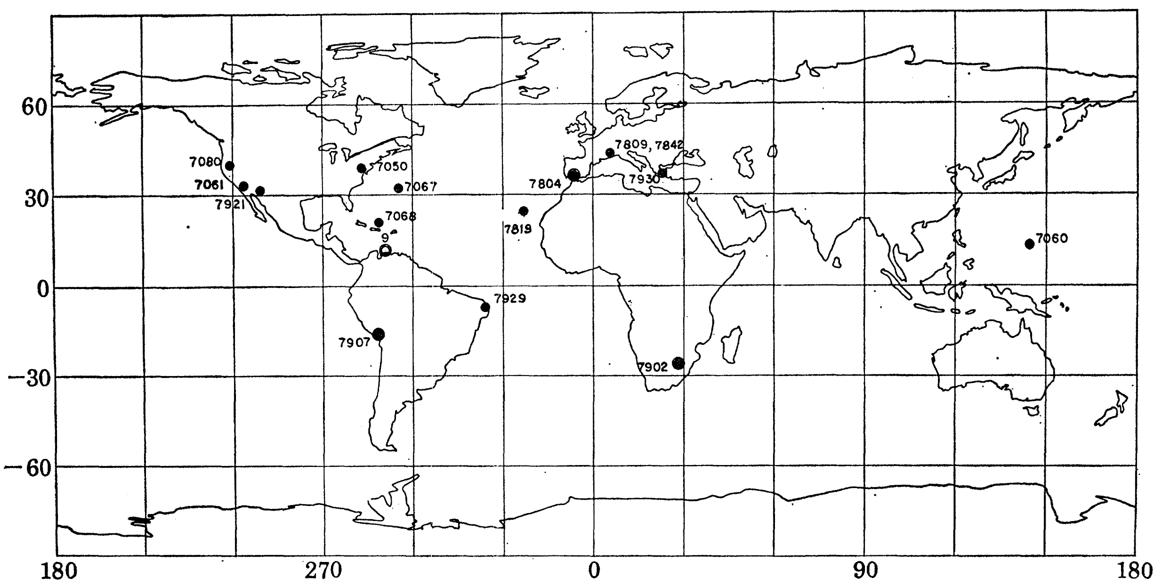

Figure 1. Locations of the observing stations included in SE IV.1.

PHILOSOPHICAL TRANSACTIONS OF THE ROYAL SOCIETY A MATHEMATICAL, PHYSICAL & ENGINEERING SCIENCES

2. Data used

The laser range data have been provided by the laser networks of the Smithsonian Astrophysical Observatory (SAO), the National Aeronautics and Space Administration's Goddard Space Flight Center (NASA/GSFC), and the Centre National d'Etudes Spatiales (CNES). These data have been acquired from the stations listed in table 2 and plotted in figure 1. The accuracy has improved from 5 m in 1971 to 5 cm for some data taken in 1975 (Gaposchkin 1974; Pearlman, Lehr, Lanham & Wohn 1975). The data are used with given *a priori* weights established from discussions with the originating agencies. The nine satellites for this analysis are given in table 3, together with their orbital characteristics. The terrestrial gravimetry data employed in this solution, when averaged to 550 km × 550 km area means, cover 86 % of the globe. The distribution of 1° × 1° area means used is shown in figure 2. The accuracy of the gravity anomalies is discussed in Williamson & Gaposchkin (1973, 1975). The simultaneous camera data and the Deep Space Net (DSN) data used to orient the coordinate reference system are described in Gaposchkin, Latimer & Veis (1973) and Gaposchkin (1974).

Table 3. Summary of dynamical data

satellite				perigee height	a	number of arcs		
designation	name	inclination (deg)	eccentricity	km	km	SE IV.1	SE IV.2	SE IV.3
6406401	BE-B	80	0.012	912	7362	2	2	2
6503201	BE-C	41	0.026	941	7311	9	9	16
6508901	Geos 1	59	0.073	1121	8074	14	14	19
6701101	D1C	40	0.052	579	7336	2	2	2
6701401	D1D	39	0.053	569	7337	3	3	3
6800201	Geos 2	105	0.031	1101	7709	8	8	13
7010901	Peole	15	0.017	635	7070	5	5	5
7501001	Starlette	50	0.0207	805	7335	5	5	5
7502701	Geos 3	115	0.0005	840	7222	—	4	6
					total	48	52	71

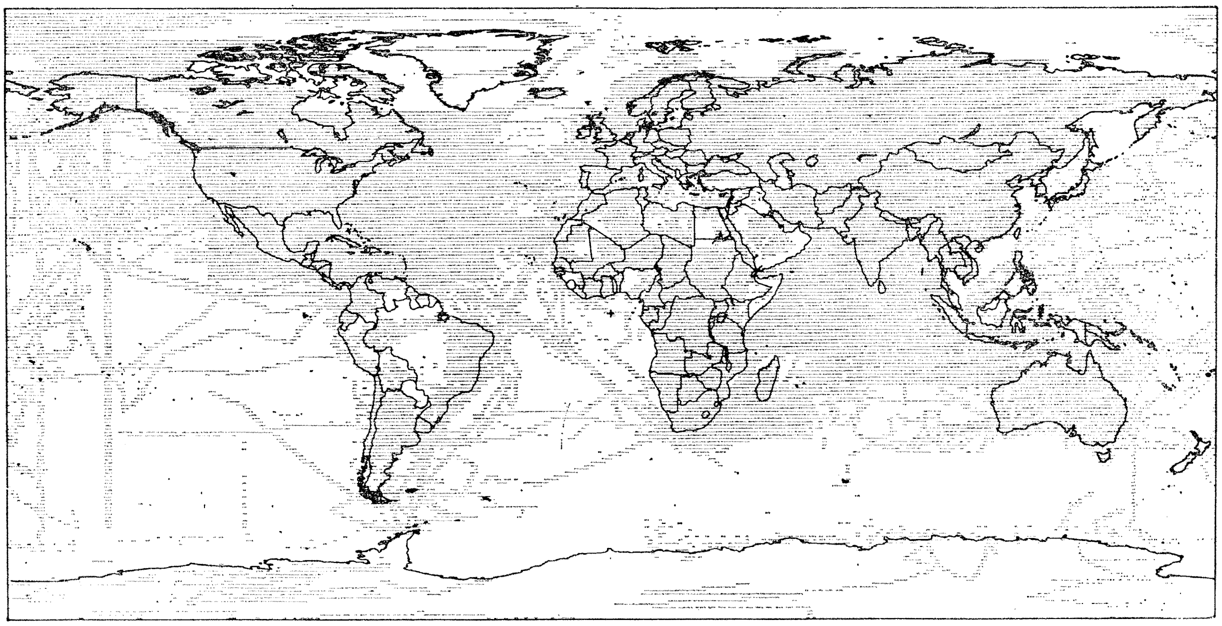

Figure 2. Distribution of 1° × 1° mean surface-gravity data.

3. Gravity-field determination

The basic approach to the determination of the gravity field through analysis or orbital perturbations is given in Gaposchkin (1973). The essential points are three in number:

(1) The satellite acts as a filter, selecting certain combinations of spherical harmonics and transforming the spatial variation of the gravity field into a periodic temporal variation in satellite position; that is, only a subset of the coefficients can be determined, and each satellite provides a unique set of frequencies.

(2) The sensitivity of a satellite decreases with degree and order. Therefore, a satellite provides the most accurate information for lower degree coefficients.

(3) To obtain a proper separation of the spherical-harmonics coefficients, a variety of orbital characteristics is necessary.

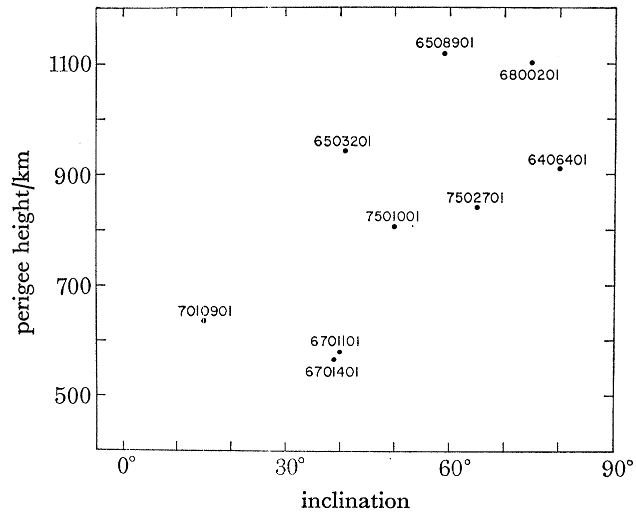

Figure 3. Distribution of perigee heights and inclinations of the satellites used in SE IV.1.

Therefore, terrestrial gravity data are used to provide information for weakly or undetermined coefficients, and a variety of satellite inclinations are chosen. The distribution of satellite inclinations is illustrated in figure 3.

From these nine satellites, 296 coefficients have been determined out of the complete 24th-degree-and-order field. The orbital data are chosen to give a distribution in inclination and height and an orbital arc length that covers at least one complete oscillation of the tesseral resonance. The orbital arcs chosen are between 10 and 20 days in length, depending also on the actual distribution of the tracking data.

The solution presented here is an update from the *1973 Smithsonian Standard Earth* (*III*) (SE III) (Gaposchkin 1973). In this nonlinear iterative process, three iterations have been completed. The first is discussed by Gaposchkin & Williamson (1975) and the second by Gaposchkin (1975). This third iteration has been computed complete through degree and order 24 and is listed in table 4. The gravity anomalies derived from these coefficients are plotted in figure 4. The tracking data were given a weight as described above, and the surface-gravity data were given a variance of

$$\sigma^2 = \frac{144}{n}\frac{\langle A \rangle}{A}\,\mathrm{mGal}^2,$$

where n is the number of $1^\circ \times 1^\circ$ squares in each $5^\circ \times 5^\circ$ mean, A is the area of the gravity anomaly, and $\langle A \rangle$ is the average area. For unobserved areas, an estimate of $\Delta g = 0$ with a variance of $\sigma^2 = 144 \langle A \rangle / A$ was used.

Three tests of the gravity field have been performed:

(1) Comparison of surface-gravity data.

(2) Comparison of satellite orbital residuals.

(3) Comparison with satellite-to-sea-surface radar altimeter data.

Assuming the solution is statistically independent of the surface-gravity data, which is not strictly true, the following quantities defined by Kaula (1966) can be computed and used to compare a geopotential model (g_s) with observed values of surface gravity (g_t):

$\langle g_t^2 \rangle$ The mean value of g_t^2, where g_t is the mean free-air gravity anomaly based on surface gravity, indicating the amount of information contained in the surface-gravity anomalies.

$\langle g_s^2 \rangle$ The mean value of g_s^2, where g_s is the mean free-air gravity anomaly computed from the geopotential model, indicating the amount of information in the computed gravity anomalies.

$\langle g_t g_s \rangle$ An estimate of g_t – i.e. the true value of the contribution to the gravity anomaly of the geopotential model and the amount of information common to both g_t and g_s.

$\langle (g_t - g_s)^2 \rangle$ The mean square difference of g_t and g_s.

$E(\epsilon_s^2)$ The mean square error in the geopotential model.

$E(\epsilon_t^2)$ The mean square error of the observed gravity.

$E(\delta g^2)$ The mean square of the error of omission – that is, the difference between true gravity and g_h; this term is then the model error.

If the geopotential model were perfect, then $\langle g_s^2 \rangle = \langle g_t^2 \rangle$, which in turn would equal $\langle g_t g_s \rangle$ if g_t were free from error and known everywhere. Then, ϵ_s^2 would be zero even though g_s would not contain all the information necessary to describe the total field. The information not contained in the model field – i.e. the error of omission, δg – then consists of the higher order coefficients. The quantity $\langle (g_t - g_s)^2 \rangle$ is a measure of the agreement between the two estimates g_t and g_s and is equal to

$$\langle (g_t - g_s)^2 \rangle = E(\epsilon_s^2) + E(\epsilon_t^2) + E(\delta g^2).$$

Another estimate of g_t can be obtained from the gravimetric estimates of degree variance σ_l^2 (Kaula 1966):

$$E(g_t^2) = D = \sum_l \frac{n_l}{2l+1} \sigma_l^2,$$

where n_l is the number of coefficients of degree l included in g_h, and

$$\sigma_l^2 = \gamma^2 (l-1)^2 \sum_m (\bar{C}_{lm}^2 + \bar{S}_{lm}^2).$$

We also have

$$E(\epsilon_s^2) = \langle g_s^2 \rangle = \langle g_s g_t \rangle$$

and

$$E(\epsilon_t^2) = \langle g_t^2 \rangle / \langle n \rangle.$$

These values are given in table 5 for SE III; for the first iteration, SE IV.1, which includes terms to 18th degree; for SE IV.1 extended to 24th degree, SE IV.1ex; for a second iteration, SE IV.2; and for the solution reported here, SE IV.3. The information content of the surface-gravity-data solution $\langle g_t^2 \rangle$ has increased in the revised set of gravity anomalies used here. This is reasonable; since the unobserved areas have an expected value of zero, the fewer observations there are, the lower the variance is. However, the information in the 18th-degree satellite solution $\langle g_s^2 \rangle$ has decreased, a fact confirmed by a decrease in D. Therefore, the information in SE III was too high. The residual $\langle (g_t - g_s)^2 \rangle$ has remained roughly the same, while the information in the higher harmonics is estimated to be larger. The estimate of $E(\epsilon_s^2)$ cannot be reliable, as the sets of data g_s and g_t are not independent.

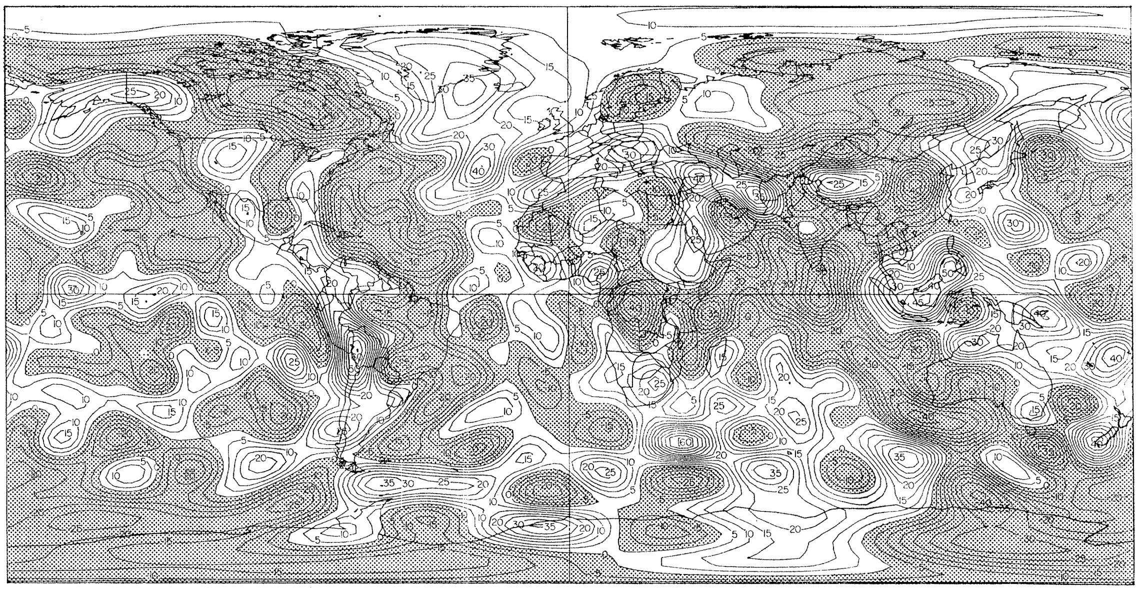

FIGURE 4. Gravity-anomaly plot from SE IV.3 for l, $m \leqslant 24$, for a best-fitting ellipsoid $1/f = 298.256$, $a_e = 6.378136 \times 10^6$ m.

TABLE 5. COMPARISON OF SURFACE GRAVITY WITH SOLUTIONS (mGal²)

solution	$l \leqslant$	$\langle (g_t - g_s)^2 \rangle$	$\langle g_t g_s \rangle$	$\langle g_s^2 \rangle$	D	$\langle g_t^2 \rangle$	$E(\epsilon_s^2)$	$E(\epsilon_t^2)$	$E\delta(g^2)$	$n \geqslant$	no. of anomalies
SE III	18	191	173	226	235	310	54	18	120	1	1474
	18	146	201	231	235	318	30	15	102	10	1158
	18	142	231	246	235	358	15	15	112	20	757
SE IV.1	18	146	190	216	224	310	26	18	102	1	1474
	18	109	218	227	224	318	9	15	85	10	1158
	18	107	247	242	224	358	−5	15	97	20	757
SE IV.1ex	24	133	214	250	283	310	36	18	79	1	1474
	24	90	242	256	283	318	14	15	61	10	1158
	24	82	275	274	283	358	−1	15	68	20	757
SE IV.2	24	109	221	241	264	310	20	18	71	1	1474
	24	76	245	246	264	318	2	15	59	10	1158
	24	72	277	267	264	358	−9	15	67	20	757
SE IV.3	24	104	222	237	251	310	16	18	71	1	1474
	24	76	244	246	251	318	2	15	59	10	1158
	24	72	277	268	251	358	−9	15	67	20	757

In table 6, an estimate of the orbital accuracy and its change with each solution is given. One arc is selected from each satellite as a test for each solution. The table lists the standard error of unit weight σ and the number of observations N used in the arc. The data for these arcs, taken from the Earth Physics Satellite Observation Campaign and the Geos 3 programme, were not

PHILOSOPHICAL TRANSACTIONS OF THE ROYAL SOCIETY A MATHEMATICAL, PHYSICAL & ENGINEERING SCIENCES

TABLE 4. TESSERAL-HARMOMICS COEFFICIENTS, C_{lm} AND S_{lm}, FOR SOLUTION SE IV. 3

Note: The coefficients are those of spherical harmonics normalized so that the integral of the square of an harmonic over a unit sphere is 4π.

l	m	$10^6 C_{lm}$	$10^6 S_{lm}$	l	m	$10^6 C_{lm}$	$10^6 S_{lm}$	l	m	$10^6 C_{lm}$	$10^6 S_{lm}$
2	2	2.41850	−1.42170	19	3	−0.00389	−0.02580	9	7	−0.19141	−0.08405
3	3	0.66522	1.48860	19	6	0.03889	0.05414	10	1	0.07963	−0.07113
4	3	1.00450	−0.19285	19	9	−0.04461	0.00116	10	4	−0.01031	−0.12082
5	2	0.61230	−0.33841	19	12	0.01314	0.00990	10	7	0.04185	0.00801
5	5	0.09713	−0.57910	19	15	−0.01208	−0.02020	10	10	0.10663	0.00754
6	3	−0.00376	0.05841	19	18	0.05479	0.00722	11	3	−0.03543	−0.22653
6	6	0.01281	−0.27466	20	2	0.00450	0.01545	11	6	−0.00616	−0.00118
7	3	0.24411	−0.24812	20	5	−0.00880	0.01412	11	9	0.00755	0.12648
7	6	−0.27061	0.15350	20	8	−0.00070	0.05417	12	1	−0.07135	−0.04250
8	2	0.08150	0.00983	20	11	0.03074	−0.01572	12	4	−0.09396	−0.06455
8	5	0.03689	0.00195	20	14	0.01732	−0.02665	12	7	−0.09239	0.02294
8	8	−0.17931	0.10295	20	17	−0.00615	−0.01765	12	10	−0.01589	−0.00949
9	3	−0.18900	−0.05918	20	20	0.00259	−0.00981	13	1	−0.05227	−0.01785
9	6	0.05800	0.19442	21	3	−0.00959	0.01764	13	4	0.01011	0.04026
9	9	−0.00254	0.04101	21	6	−0.00016	0.00556	13	7	0.02348	0.07551
10	3	−0.07161	−0.06977	21	9	−0.02278	0.02433	13	10	0.01766	−0.02996
10	6	−0.02410	−0.10872	21	12	0.01513	−0.00214	13	13	−0.04858	0.08088
10	9	0.08490	−0.01824	21	15	0.00974	0.00301	14	3	0.03016	−0.02494
11	2	−0.07709	−0.07450	21	18	0.03111	0.00854	14	6	0.01341	0.04053
11	5	0.00597	0.00742	21	21	0.00524	−0.00162	14	9	0.01602	0.10555
11	8	0.05583	0.02720	22	3	0.02292	0.00780	14	12	0.00273	−0.01985
11	11	0.09096	−0.01344	22	6	0.00815	−0.02002	15	1	0.04541	0.02027
12	3	0.06967	0.11387	22	9	0.02241	0.01681	15	4	−0.03462	0.04118
12	6	0.01362	0.01897	22	12	−0.02693	0.00391	15	7	0.10339	0.09337
12	9	−0.03408	0.06251	22	15	0.02335	0.00398	15	10	−0.06956	0.00901
12	12	0.01389	0.01817	22	18	0.02260	−0.00276	15	13	−0.00609	0.00308
13	3	−0.03670	0.06864	22	21	−0.02825	0.02853	16	1	0.01616	0.05647
13	6	−0.07322	0.02257	23	2	0.00133	−0.02053	16	4	0.05737	0.04996
13	9	0.00520	0.03576	23	5	0.03222	0.00620	16	7	−0.02372	−0.04542
13	12	−0.01797	0.10403	23	8	0.00694	0.00243	16	10	0.01630	−0.04265
14	2	−0.02871	−0.00347	23	11	−0.00574	0.01711	16	13	0.00336	−0.00943
14	5	−0.02149	−0.02613	23	14	0.01750	−0.02136	16	16	−0.02052	−0.00242
14	8	−0.04395	−0.04641	23	17	−0.01571	−0.01680	17	3	0.01160	0.00402
14	11	0.00717	−0.05827	23	20	−0.00400	−0.00033	17	6	−0.03366	−0.04151
14	14	−0.05630	−0.00322	23	23	−0.01048	−0.01981	17	9	−0.04467	−0.06275
15	3	0.05344	0.03729	24	3	−0.01051	−0.01285	17	12	0.02902	0.01431
15	6	−0.00988	−0.07868	24	6	−0.00684	−0.00238	17	15	0.02580	0.02138
15	9	−0.01462	0.02599	24	9	−0.04896	−0.00946	18	1	−0.01264	−0.03310
15	12	−0.00950	0.03440	24	12	0.02427	−0.01869	18	4	0.05267	0.01406
15	15	−0.03348	0.03635	24	15	0.00597	−0.00762	18	7	0.02064	−0.02277
16	3	−0.03314	−0.00495	24	18	0.00909	0.00021	18	10	0.03372	−0.01729
16	6	0.00634	−0.03827	24	21	−0.01030	0.02316	18	13	−0.01080	−0.04457
16	9	0.02029	−0.04059	24	24	0.00821	−0.00973	18	16	0.01519	0.00127
16	12	−0.01034	0.00709	27	13	0.01536	−0.03544	19	1	−0.02178	0.01663
16	15	−0.01652	−0.05836	3	1	2.04910	0.27700	19	4	−0.00193	−0.03373
17	2	−0.02454	0.02305	4	1	−0.58428	−0.46844	19	7	−0.01290	−0.01412
17	5	−0.03944	0.02060	4	4	−0.09033	0.27706	19	10	−0.03573	−0.01619
17	8	0.04479	−0.03289	5	3	−0.58737	−0.05459	19	13	0.01701	−0.00502
17	11	0.07356	0.04451	6	1	−0.07823	0.01839	19	16	−0.02254	−0.01492
17	14	−0.01373	0.01322	6	4	−0.04001	−0.37027	19	19	−0.02174	0.00660
17	17	−0.06590	−0.00144	7	1	0.26053	0.06631	20	3	0.01323	0.00436
18	3	−0.02590	0.00726	7	4	−0.14505	−0.17486	20	6	0.02501	−0.02063
18	6	−0.02321	−0.03044	7	7	0 04432	−0.09185	20	9	0.08565	−0.01039
18	9	0.03822	0.01641	8	3	−0.04088	−0.02498	20	12	−0.05473	−0.03269
18	12	−0.05544	−0.01729	8	6	−0.12014	0.21447	20	15	−0.01100	−0.01564
18	15	−0.04883	−0.00401	9	1	0.17280	−0.02036	20	18	−0.00306	−0.02031
18	18	−0.00454	−0.00329	9	4	−0.08453	0.04620	21	1	−0.00388	0.03466

TABLE 4 (*cont.*)

l	m	$10^6 C_{lm}$	$10^6 S_{lm}$	l	m	$10^6 C_{lm}$	$10^6 S_{lm}$	l	m	$10^6 C_{lm}$	$10^6 S_{lm}$
21	4	−0.01577	0.03553	9	8	0.22047	−0.01327	19	5	−0.02442	−0.01754
21	7	−0.03586	−0.01373	10	2	−0.06514	0.00802	19	8	0.04724	−0.01829
21	10	−0.00845	−0.03219	10	5	−0.01777	0.02161	19	11	0.01822	0.06430
21	13	0.02005	0.03340	10	8	0.05510	−0.09175	19	14	−0.00317	−0.00436
21	16	0.00743	−0.01346	11	1	−0.00328	0.01680	19	17	0.06154	−0.01856
21	19	−0.05060	0.00289	11	4	−0.09886	−0.10843	20	1	−0.00850	−0.03348
22	1	0.01214	0.00347	11	7	0.05265	−0.03807	20	4	−0.00762	−0.03487
22	4	0.01749	−0.00572	11	10	−0.05558	0.02544	20	7	−0.01581	0.01790
22	7	0.00273	0.05570	12	2	0.03148	−0.02717	20	10	−0.01207	0.00744
22	10	0.00193	0.04487	12	5	0.04100	0.03248	20	13	0.04112	0.02014
22	13	−0.02258	0.00066	12	8	−0.00777	0.05503	20	16	0.00069	0.00394
22	16	−0.01334	−0.00055	12	11	−0.00282	0.01727	20	19	−0.00444	0.00110
22	19	0.03157	0.00076	13	2	0.00795	−0.05381	21	2	0.01227	−0.01142
22	22	−0.00984	−0.00140	13	5	0.11180	0.04126	21	5	0.03139	−0.04049
23	3	−0.01591	−0.02863	13	8	0.00567	−0.04582	21	8	0.02815	−0.00081
23	6	−0.03038	0.03683	13	11	−0.04234	0.04537	21	11	0.00533	−0.03548
23	9	0.01674	0.01326	14	1	0.01457	0.02307	21	14	0.00954	0.01405
23	12	0.01647	−0.00543	14	4	0.01208	−0.05915	21	17	0.00339	0.01443
23	15	0.01484	0.00256	14	7	0.00115	−0.09597	21	20	−0.02022	0.03386
23	18	0.01278	−0.00907	14	10	0.03359	−0.04565	22	2	−0.01173	0.01705
23	21	0.01946	−0.00221	14	13	0.03265	0.04509	22	5	−0.03021	0.03688
24	1	−0.01376	0.00549	15	2	0.00604	−0.03512	22	8	−0.03771	0.00126
24	4	−0.00746	0.02529	15	5	0.04412	0.02846	22	11	0.00569	−0.02600
24	7	0.00967	−0.00726	15	8	−0.01663	0.03337	22	14	−0.00082	0.00665
24	10	0.03325	0.01903	15	11	0.03335	0.02008	22	17	0.02599	−0.03734
24	13	−0.01173	−0.00559	15	14	0.00482	−0.03382	22	20	−0.00612	0.01411
24	16	0.00770	0.00635	16	2	−0.01190	−0.00320	23	1	0.00600	0.03368
24	19	−0.03158	0.00447	16	5	−0.01876	0.00518	23	4	−0.00764	0.01446
24	22	−0.00316	−0.01505	16	8	−0.05528	0.04268	23	7	−0.00899	−0.01315
25	13	0.01139	0.00318	16	11	0.00003	−0.02050	23	10	0.00325	−0.00257
27	14	0.01717	−0.05403	16	14	−0.02010	−0.03331	23	13	0.01279	0.00645
3	2	0.91763	−0.68102	17	1	−0.03409	−0.04676	23	16	0.02042	−0.00949
4	2	0.35756	0.63501	17	4	−0.06372	0.03890	23	19	−0.00031	0.00984
5	1	−0.08500	−0.11014	17	7	0.04450	0.01072	23	22	−0.01419	0.01793
5	4	−0.28573	0.00526	17	10	0.00247	0.02897	24	2	−0.00301	0.01632
6	2	0.08701	−0.43707	17	13	0.02055	0.04389	24	5	−0.03199	−0.01342
6	5	−0.28476	−0.46418	17	16	−0.04377	0.01812	24	8	0.01602	−0.02357
7	2	0.27311	0.13678	18	2	−0.01735	0.01829	24	11	0.01333	0.03002
7	5	0.02508	0.03487	18	5	0.02412	−0.01093	24	14	−0.04424	0.02837
8	1	0.00865	0.02621	18	8	−0.00724	0.01531	24	17	−0.01959	−0.00238
8	4	−0.17405	0.07901	18	11	−0.05602	−0.00013	24	20	−0.01070	0.01233
8	7	0.08145	0.11022	18	14	0.00061	−0.02720	24	23	0.00734	−0.01529
9	2	−0.01486	−0.07874	18	17	0.01243	−0.00594	25	14	−0.02210	0.02149
9	5	−0.12391	−0.00321	19	2	0.02950	0.01465				

used in the computation of SE III. The test arcs for Starlette (7501001) and Geos 3 (7502701) were changed for the third iteration. The particularly large initial uncertainty for Starlette and Geos 3 is largely due to some specific resonance terms; once these were identified, the uncertainties came down to a reasonable level. Peole (7010901) is used as the ultimate test for a gravity field; because of its low altitude and low inclination, it supplies relatively few data and the orbits are not so accurate. We continue to believe that it does give a positive contribution to our knowledge of the geopotential.

Satellite-to-sea-surface altimeter data provide a combined test of the ephemeris accuracy and the geopotential. Figure 5 is a plot of the absolute residuals for one track of Geos 3 altimetry data. The satellite ephemeris is computed from laser tracking data, and the geoid is defined with this solution truncated at 18th degree and order. The residuals are consistent with an orbital accuracy of 5 m, a geoid accuracy of 3 m, and an altimeter accuracy of better than 1 m.

Table 6. Comparison of solutions (standard error of unit weight and number of observations)

solution	no. of arcs in solution	l_{max}	surface gravity $\langle(g_t-g_s)^2\rangle$ (mGal²) $n>1$	$n>10$	$n>20$	Geos 1 σ	N	BE-C σ	N	Geos 2 σ	N	Starlette σ	N	Peole σ	N	Geos 3 σ	N
$GM = 3.986013\times10^{20}$ cm³ s⁻²																	
SE III	203	18	191	146	142	4.53	3021	5.81	1699	5.58	1112	16.61	2443	15.41	805	13.16	1076
SE IV.1	52	18	146	109	107	3.72	3022	4.52	1695	3.13	1122	5.12	2258	11.38	794	11.37	1078
SE IV.2	52	24	109	76	72	3.66	3023	3.86	1689	3.01	1124	*3.15*	*2274*	12.56	814	*7.24*	*1065*
$GM = 3.986005\times10^{20}$ cm³ s⁻²																	
SE IV.2	52	24	109	76	72	4.59	3053	4.97	1701	3.51	1132	6.50	1645	11.55	811	11.31	1770
SE IV.3†	71	24	127	95	90	4.18	3028	3.48	1645	3.95	1147	5.85	1643	10.78	509	10.33	1769

† Improved coordinates.

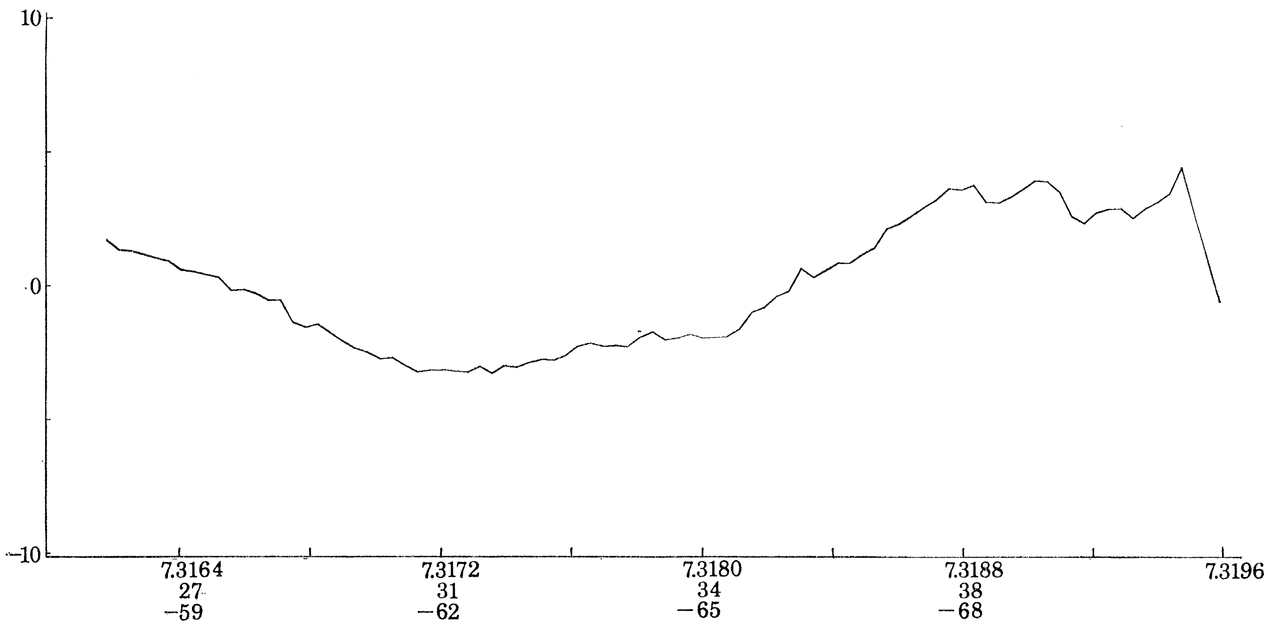

Figure 5. Altimeter residuals with respect to the 18th-degree field (SE IV.3).

4. Station-coordinate determination

The station coordinates were determined in parallel in this third iteration. Laser range measurements are invariant under translation and rotation of the reference system, and so we have no obvious relation to a defined system. The satellite theory with $C_{21} = S_{21} = J_1 = 0$ is referred to the Earth's centre of mass and the Conventional International Origin through observations of pole position. Therefore, if temporal variations such as tides are properly modelled, centre-of-mass coordinates should be realized. However, the longitude origin will be arbitrary. We then look to observations from camera and deep-space probes to provide this orientation. An individual station position in a geometrical network, such as the Baker–Nunn (Gaposchkin 1974) or the BC-4 (Schmid 1974), may not approach 1 m; however, the mean system could provide orientation to that accuracy (Gaposchkin 1974; Mueller 1974). We therefore combine the geometrical network in such a way that the relative positions of the laser stations are preserved and the orientation of the resulting system is the FK4 system defined by U.T. 1 and by pole-position values determined by the Bureau International de l'Heure. Ultimately, the orientation in longitude could come from the DSN coordinates, which could be related to the FK4 system with greater accuracy through the use of planetary ephemerides. We have included the data from the DSN allowing for such a rotation. Table 7 gives the adjusted coordinates for all the stations.

The combination solution provides for orientation differences and for a scale difference for the DSN, both of which are consistent with the results in SE III. The scale difference for the DSN is due to the change of length scale defined by the adopted value of GM (table 1).

Tests of station coordinates include (1) a comparison of orbital residuals and (2) a comparison of ellipsoid heights.

The orbital residuals are given in table 6. The orbital accuracy is consistent with a 3–5 m accuracy in the station coordinates.

The height above the ellipsoid for a station can be estimated by summing the mean sea-level height h_{msl} and the geoid height N and can be compared with the ellipsoid height (h_e) determined from the geocentric coordinates. The error Δh is

$$\Delta h = h_e - h_{msl} - N.$$

We can obtain N from the spherical-harmonics coefficients in table 4. The mean change Δh is, of course, a change in the semidiameter of the reference ellipsoid, a_e, whose revised value,

$$a_e = (6.378136 \pm 1)\ \mathrm{Mm},$$

obtained from a weighted mean of all 114 stations, is consistent with the change in GM of 2 parts per 3 million.

5. Discussion

The most obvious result from the new laser data is the increased capability for determining the long-wavelength features of the Earth's gravity field. The desired signal (5–10 m) is far above the noise in the data (5–10 cm). Some coefficients of the gravity field must be determined from terrestrial gravimetry, but these will soon be derived by satellite-altimeter data and satellite-to-satellite tracking data. Significant improvement still remains to be obtained from the laser data now in hand and currently being acquired. However, important geophysical phenomena must also be modelled and determined. For example, the effects of solid-earth, ocean, and atmospheric

TABLE 7. CORRECTED STATION COORDINATES FOR SE. VI. 3

Note: X, Y, Z are geocentric rectangular co-ordinates. The axes of X and Y lie in the equatorial plane, with X in the meridian of Greenwich. Z is positive in the direction of the North Pole. The units of X, Y and Z are 10^6 m.

station number	X	Y	Z	σ/m	location	station number	X	Y	Z	σ/m	location
1021	1.1180419	−4.8763121	3.9429737	2.2	Blossom Point, U.S.A.	6020	−1.8885957	−5.3548751	−2.8957500	12.2	Easter Is., Chile
1022	0.8078777	−5.6519616	2.8334964	6.0	Ft. Myers, U.S.A.	6022	−6.0999533	−0.9973364	−1.5685863	8.6	Tutuila, Am. Samoa
1030	−2.3572308	−4.6463134	3.6683199	6.1	Goldstone, U.S.A.	6023	−4.9553563	3.8422645	−1.1638574	6.4	Thursday Is., Australia
1034	−0.5216929	−4.2420613	4.7187462	6.3	East Grand Fork, U.S.A.	6031	−4.3138011	0.8913557	−4.5972716	6.9	Invercargill, New Zealand
1042	0.6475288	−5.1779169	3.6567070	4.3	Rosman, U.S.A.	6032	−2.3753830	4.8755656	−3.3453999	7.9	Caversham, Australia
1055	3.9073919	1.6024471	4.7639259	7.8	Uzhgorod, U.S.S.R.	6038	−2.1609729	−5.6426966	2.0353602	5.3	Revilla Gigedo, Mexico
1072	2.8862402	2.1559923	5.2459136	23.9	Zvenigorod, U.S.S.R.	6039	−3.7247516	−4.4212135	−2.6860880	13.5	Pitcairn Is., U.K.
1084	3.1838714	1.4214952	5.3228066	7.9	Riga, Latvia	6040	−0.7419540	6.1908067	−1.3385572	8.5	Cocos Is., Australia
1113	4.1842393	1.4376943	4.5793082	12.8	Baja, Hungary	6042	4.9007581	3.9682566	0.9663253	5.9	Addis Ababa, Ethiopia
1131	4.0986239	2.0077459	4.4411900	64.9	Bucharest, Rumania	6043	1.3713891	−3.6147475	−5.0559454	8.6	Cerro Sombrero, Chile
1147	3.9784445	1.0510658	4.8575560	9.9	Ondrejov, Czechoslavakia	6044	1.0989150	3.6846448	−5.0718735	14.3	Heard Is., Australia
1181	3.8006249	0.8819794	5.0288679	31.5	Potsdam, G.D.R.	6045	3.2234456	5.0453464	−2.1918063	6.2	Mauritius, U.K.
1901	4.7282961	2.8796833	3.1568001	16.5	Helwan, Egypt	6047	−3.3619323	5.3658236	0.7636181	9.1	Zamboanga, Philippines
4711	−2.3514438	−4.6450713	3.6737634	2.4	California J.P.L., U.S.A.	6050	1.1926919	−2.4509935	−5.7470533	12.3	Palmer Sta., Antarctic
4712	−2.3504573	−4.6519707	3.6656283	2.4	California J.P.L., U.S.A.	6051	1.1113520	2.1692761	−5.8743464	8.6	Mawson Sta., Antarctic
4714	−2.3536360	−4.6413339	3.6770517	2.4	California J.P.L., U.S.A.	6052	−0.9025774	2.4095468	−5.8165640	8.9	Wilkes Sta., Antarctic
4741	−3.9787053	3.7248595	−3.3021942	5.7	Australia J.P.L.	6053	−1.3108226	0.3112806	−6.2132898	8.6	McMurdo Sta., Antarctic
4742	−4.4609688	2.6824262	−3.6745997	6.5	Australia J.P.L.	6055	6.1183440	−1.5717290	−0.8786171	6.7	Ascension Is., U.K.
4751	5.0854485	2.6682510	−2.7687110	3.3	So. Africa J.P.L.	6059	−5.8853314	−2.4483506	0.2216717	8.2	Christmas Is., U.K.
4761	4.8492410	−0.3602940	4.1148628	3.8	Spain J.P.L.	6060	−4.7516240	2.7920850	−3.2001674	5.7	Culgoora, Australia
4762	4.8466986	−0.3702118	4.1168859	3.8	Spain J.P.L.	6061	2.9999343	−2.2193572	−5.1552594	9.7	So. Georgia, U.K.
6001	0.5465824	−1.3899725	6.1802327	6.8	Thule, Greenland	6063	5.8844814	−1.8534765	1.6128467	6.8	Daker, Senegal
6002	1.1307801	−4.8308268	3.9947011	2.2	Beltsville, U.S.A.	6064	6.0234014	1.6179516	1.3317224	6.3	Fort Lamy, Chad
6003	−2.1278215	−3.7858447	4.6560322	4.5	Moses Lake, U.S.A.	6065	4.2135809	0.8208526	4.7027644	7.6	Hohenpeissenberg, W. Germany
6004	−3.8517740	0.3964309	5.0513396	12.0	Shemya, U.S.A.	6067	5.1864102	−3.6539246	−0.6542927	2.6	Natal, Brazil
6006	2.1029456	0.7216929	5.9581750	8.0	Tromso, Norway	6068	5.0848501	2.6703491	−2.7680996	2.2	Johannesburg, Rep. S. Afr.
6007	4.4336553	−2.2681269	3.9716442	7.7	Azores, Portugal	6069	4.9784433	−1.0868595	−3.8231669	16.0	Tristan Da Cunha, U.K.
6008	3.6232539	−5.2142244	0.6015282	8.1	Paramaribo, Netherland	6072	−0.9416778	5.9674633	2.0393000	9.1	Chiang Mai, Thailand
6009	1.2808525	−6.2509404	−0.0108140	9.4	Quito, Ecuador	6073	1.9051513	6.0322890	−0.8107375	7.8	Chagos, Archipelago
6011	−5.4660225	−2.4044070	2.2422174	7.7	Maui, U.S.A.	6075	3.6028323	5.2382481	−0.5159534	7.7	Seychelles, U.K.
6012	−5.8585389	1.3945249	2.0937977	9.3	Wake Is., U.S.A.	6078	−5.9523058	1.2319329	−1.9259372	16.6	New Hebrides, U.K.
6013	−3.5658560	4.1207355	3.3034157	10.0	Kanoya, Japan	6111	−2.4488455	−4.6679697	3.5827501	2.2	Wrightwood, U.S.A.
6015	2.6043682	4.4441756	3.7503106	6.8	Mashhad, Iran	6123	−1.8817858	−0.8124140	6.0195916	10.4	Point Barrow, U.S.A.
6016	4.8964065	1.3161948	3.8566635	6.7	Catania, Italy	6134	−2.4488994	−4.6680601	3.5824449	2.1	Wrightwood, U.S.A.
6019	2.2806410	−4.9145431	−3.3554179	5.5	Villa Dolores, Argentina	7036	−0.8284805	−5.6574332	2.8168006	6.6	Edinburg, U.S.A.

PHILOSOPHICAL TRANSACTIONS OF THE ROYAL SOCIETY A MATHEMATICAL, PHYSICAL & ENGINEERING SCIENCES

Table 7 (*cont.*)

station number	X	Y	Z	σ/m	location
7037	−0.1912756	−4.9672788	3.9832630	3.9	Columbia, U.S.A.
7039	2.3082388	−4.8735837	3.3945837	5.1	Bermuda
7040	2.4650687	−5.5348833	1.9855153	10.1	San Juan, Puerto Rico
7043	1.1307228	−4.8313144	3.9941447	6.5	Greenbelt, U.S.A.
7045	−1.2404649	−4.7602301	4.0489940	5.0	Denver, U.S.A.
7050	1.1306854	−4.8313643	3.9941018	2.0	Greenbelt, U.S.A.
7060	−5.0689510	3.5840978	1.4587745	13.9	Guam, U.S.A.
7061	−2.4288433	−4.7997481	3.4172727	2.0	San Diego, U.S.A.
7063	1.1307075	−4.8313748	3.9940848	2.0	Greenbelt, U.S.A.
7067	2.3085388	−4.8740827	3.3936237	5.1	Bermuda
7068	1.9204830	−5.6194852	2.3189149	5.0	Grand Turk
7072	0.9762902	−5.6013787	2.8802388	5.7	Jupiter, U.S.A.
7075	0.6926439	−4.3470684	4.6004998	6.7	Sudbury, Ontario, Canada
7076	1.3841912	−5.9056301	1.9665265	10.4	Kingston, Jamaica
7080	−2.5169080	−4.1988374	4.0764075	2.3	Quincy, U.S.A.
7804	5.1056143	−0.5552477	3.7696289	3.9	San Fernando, Spain
7809	4.5783427	0.4579879	4.4031646	5.1	Haute Provence, France
7819	5.4404830	−1.5016750	2.9612566	4.6	Grand Canary Is.
7842	4.5816812	0.5562044	4.3893198	5.5	Grasse, France
7902	5.0561281	2.7165161	−2.7757732	2.0	Olifantsfontein, Rep. S. Afr.
7907	1.9427817	−5.8040866	−1.7969243	2.0	Arequipa, Peru
7921	−1.9367812	−5.0777035	3.3319144	2.0	Mt. Hopkins, U.S.A.
7929	5.1864546	−3.6538634	−0.6543299	2.4	Natal, Brazil
7930	4.5952146	2.0394687	3.9126034	4.4	Dionysos, Greece
7940	4.5952146	2.0394684	3.9126034	4.4	Dionysos, Greece
8009	4.5783652	0.4579811	4.4031426	5.1	Haute Provence, France
8010	4.3312983	0.5675437	4.6331081	5.2	Zimmerwald, Switzerland
8011	3.9201548	−0.1347215	5.0127315	7.0	Malvern, U.K.
8015	4.5783220	0.4579968	4.4031864	5.1	Haute Provence, France
8019	4.5794767	0.5866255	4.3864125	5.3	Nice, France
8034	3.9196517	0.2988586	5.0058873	8.3	Ypburg, Netherland

station number	X	Y	Z	σ/m	location
9001	−1.5357441	−5.1669895	3.4010382	5.1	Organ Pass, U.S.A.
9002	5.0561283	2.7165162	−2.7757732	2.0	Olifantsfontein, Rep. S. Afr.
9004	5.1055942	−0.5552254	3.7696602	3.9	San Fernando, Spain
9005	−3.9466965	3.3662984	3.6988226	10.4	Tokyo, Japan
9006	1.0181965	5.4711404	3.1096386	16.4	Naini Tal, India
9007	1.9427816	−5.8040862	−1.7969242	2.0	Arequipa, Peru
9008	3.3768934	4.4040025	3.1362539	12.3	Shiraz, Iran
9009	2.2518325	−5.8169047	1.3271534	6.6	Curacao, Antilles
9010	0.9763053	−5.6013809	2.8802313	5.6	Jupiter, U.S.A.
9011	2.2805892	−4.9145802	−3.3553989	5.5	Villa Dolores, Argentina
9012	−5.4660720	−2.4042880	2.2421814	7.7	Maui, U.S.A.
9021	−1.9367823	−5.0777065	3.3319092	2.0	Mt. Hopkins, U.S.A.
9022	5.0561223	2.7165269	−2.7757719	2.0	Olifantsfontein, Rep. S. Afr.
9023	−3.9777696	3.7251093	−3.3030140	5.8	Island Lagoon, Australia
9025	−3.9104401	3.3763601	3.7292094	10.4	Dodaira, Japan
9027	1.9427765	−5.8040929	−1.7969025	2.0	Arequipa, Peru
9028	4.9037504	3.9652236	0.9638629	6.0	Addis Ababa, Ethiopa
9029	5.1864544	−3.6538632	−0.6543298	2.4	Natal, Brazil
9030	4.5952057	2.0394685	3.9126133	4.4	Dionysos, Greece
9031	1.6938121	−4.1123622	−4.5566375	17.4	Comodoro Rivadavia, Argentina
9039	5.1864645	−3.6538424	−0.6543295	2.4	Natal, Brazil
9050	1.4897634	−4.4674841	4.2873186	8.1	Agassiz Station, U.S.A.
9064	3.0600427	0.9701616	5.4929921	19.3	Uppsala, Sweden
9076	2.8845316	1.3421456	5.5095272	15.0	Helsinki, Finland
9091	4.5951587	2.0394865	3.9126500	4.4	Dionysos, Greece
9113	−2.4500047	−4.6244151	3.6350322	2.2	Rosamond, U.S.A.
9114	−1.2648254	−3.4668790	5.1854380	11.4	Cold Lake, Canada
9115	3.1212815	0.5926507	5.5127023	14.8	Harestua, Norway
9117	−6.0074164	−1.1118771	1.8257380	17.6	Johnston Is., U.S.A.
9119	−4.5336624	0.7616188	−4.4077857	155.3	Mt. John, New Zealand

tides on both the gravity field and the station positions will be derived. Currently, preliminary analyses and nominal values are being employed for the reduction of data. The pole position is being monitored by classical and satellite methods now, and eventually it will be known to a few centimetres. Variations in the rotation of the Earth will become important. In addition, relative motions of the stations due to tectonic processes will be modelled and monitored with laser data. A unified coordinate system for a solution like this will provide a framework for such monitoring, although the analysis of the data will probably be done along other lines. Finally, it is an open question what reference frame must be used for analysing these observations, as is discussed in Kolaczek & Weiffenbach (1974).

6. Conclusions

Laser tracking data of decimetre accuracy can be and have been used to improve our knowledge of station coordinates and of the Earth's gravity field to degree and order 24.

The accuracy of the gravity field and station coordinates allows satellite ephemerides to be computed to better than 10 m.

Considerable more progress is possible. There seems to be no obstacle to obtaining decimetre results for orbital ephemerides and geoid height comparable to the accuracy of laser data.

More geophysical phenomena must be taken into account, and satellite data will become a source of information on tides and other deformations and on tectonic plate motion in the future.

This work was supported in part by Grant NGR 09-015-002 from the National Aeronautics and Space Administration.

References (Gaposchkin)

Aksnes, K. 1976 Short-period and long-period perturbations of a spherical satellite due to direct solar radiation. *Celest. Mech.* **13**, 89–104.

Anderle, R. J. 1974 Transformation of terrestrial survey data to doppler satellite datum. *J. geophys. Res.* **79**, 5319–5331.

Esposito, P. B. & Ng, A. T. Y. 1975 Geocentric gravitational constant determined from spacecraft radiometric data. Presented at the General Assembly of the International Association of Geodesy, Grenoble, France, August.

Gaposchkin, E. M. (ed.) 1973 *1973 Smithsonian Standard Earth (III)*. *Smithsonian Astrophys. Obs. Spec. Rep.* no. 353, 388 pp.

Gaposchkin, E. M. 1974 Earth's gravity field to the eighteenth degree and geocentric coordinates for 104 stations from satellite and terrestrial data. *J. geophys. Res.* **79**, 5377–5411.

Gaposchkin, E. M. 1975 The Smithsonian Standard Earth. Presented at the NASA Earth and Ocean Dynamics Applications Program Modeling Conference, Washington, D. C., November.

Gaposchkin, E. M., Latimer, J. & Mendes, G. 1975 Station coordinates in the Standard Earth III system and radiation-pressure perturbations from ISAGEX camera data. Presented at the General Assembly of the International Association of Geodesy, Grenoble, France, August.

Gaposchkin, E. M., Latimer, J. & Veis, G. 1973 Determination of station coordinates. In *1973 Smithsonian Standard Earth (III)* (ed. E. M. Gaposchkin). *Smithsonian Astrophys. Obs. Spec. Rep.* no. 353, pp. 309–364.

Gaposchkin, E. M. & Williamson, M. R. 1975 Revision of geodetic parameters. Presented at the General Assembly of the International Association of Geodesy, Grenoble, France, August.

Kaula, W. M. 1966 Tests and combinations of satellite determinations of the gravity fields with gravimetry. *J. geophys. Res.* **71**, 5303–5314.

Kinoshita, H. 1975 Formulas for precession. *Smithsonian Astrophys. Obs. Spec. Rep.* no. 364, 25 pp.

Kinoshita, H. 1976 Theory of the rotation of the rigid earth. Submitted to *Celest. Mech.*

Kolaczek, B. & Weiffenbach, G. (eds.) 1974 *On reference coordinate systems of Earth dynamics*. Proc. IAU Colloq. no. 26. Warsaw: Polish Acad. Sci.

Kozai, Y. 1973 A new method to compute lunisolar perturbations in satellite motions. *Smithsonian Astrophys. Obs. Spec. Rep.* no. 349, 27 pp.

Lautman, D. A. 1976*a* Perturbations of a close-earth satellite due to sunlight diffusely reflected from the earth. *Celest. Mech.* (in the press).
Lautman, D. A. 1976*b* Perturbations of a close-earth satellite due to sunlight reflected from the earth. II. Variable albedo. *Celest. Mech.* (in the press).
Lautman, D. A. 1976*c* Perturbations of a close-earth satellite due to delayed infrared emission from the earth. To be submitted to *Celest. Mech.*
Mueller, I. I. 1974 Global satellite triangulation and trilateration results. *J. geophys. Res.* **79**, 5333–5347.
Pearlman, M. R., Lehr, C. G., Lanham, N. W. & Wohn, J. 1975 The Smithsonian satellite ranging laser system. Presented at the General Assembly of the International Association of Geodesy, Grenoble, France, August.
Schmid, H. H. 1974 Worldwide geometric satellite triangulation. *J. geophys. Res.* **79**, 5349–5376.
Smith, D. E., Lerch, F. J., Marsh, J. G., Wagner, C. A., Kolenkiewicz, R. & Khan, M. A. 1975 Contributions to the National Geodetic Satellite Program by Goddard Space Flight Center. *J. geophys. Res.* **81**, 1006–1026.
Williamson, M. R. & Gaposchkin, E. M. 1973 Estimate of gravity anomalies. In *1973 Smithsonian Standard Earth (III)* (ed. E. M. Gaposchkin). *Smithsonian Astrophys. Obs. Spec. Rep.* no. 353, pp. 193–228.
Williamson, M. R. & Gaposchkin, E. M. 1975 The estimation of 550 km × 550 km mean gravity anomalies. *Smithsonian Astrophys. Obs. Spec. Rep.* no. 363, 20 pp.

Discussion

J. A. Weightman (*Geodetic Office, Elmwood Avenue, Feltham, Middlesex*). Since scale from the laser observations fails to correspond with that derived from the adopted value of *GM*, could not the explanation still lie in the calibration of the laser measures (since theoretical corrections and the measurement of relatively short distances between two terrestrial stations with all the attendant problems of refraction for terrestrial rays and of a reliable terrestrial distance do not really compare with longer field observations in space, where there are no other reliable data for direct comparison)? After all, 1.6 m on the Earth's equatorial radius is a scale difference of only 0.25 part per million.

E. M. Gaposchkin. Calibration of the laser measurements is critical, and considerable attention is given to it (Pearlman *et al.*, these proceedings). Also, systematic errors due to atmospheric refraction and to consequences of satellite design are possible. For early laser data (*ca.* 1971), systematic errors of 1–2 m are very likely. Since then, steady improvements in calibration procedures, system modelling, and component design have achieved the present state of *ca.* 15 cm pass biases. We see no problem, in principle, in making further improvement. These errors are systematic in each pass but vary from pass to pass, and we hope that they average out when taken over many passes. The refraction errors and satellite design errors are certainly less than 10 cm, except for exceptional and infrequent circumstances. Therefore, it is unlikely that scale errors of 1 m are due to calibration problems. More likely are small inconsistencies in the orbit theory used to calculate the satellite ephemeris.